



# Application of immobilized TiO<sub>2</sub> on PVDF dual layer hollow fibre membrane to improve the photocatalytic removal of pharmaceuticals in different water matrices



Lidia Paredes<sup>a</sup>, Sapia Murgolo<sup>b</sup>, Hazlini Dzinun<sup>c,d</sup>, Mohd Hafiz Dzarfan Othman<sup>c</sup>, Ahmad Fauzi Ismail<sup>c</sup>, Marta Carballa<sup>a,\*</sup>, Giuseppe Mascolo<sup>b,\*</sup>

<sup>a</sup> Department of Chemical Engineering, Instituto de Tecnología, Universidade de Santiago de Compostela, 15782 Santiago de Compostela, Spain

<sup>b</sup> CNR, Istituto di Ricerca Sulle Acque, Via F. De Blasio 5, 70132 Bari, Italy

<sup>c</sup> Advanced Membrane Technology Research Centre (AMTEC), Universiti Teknologi Malaysia, 81310 Skudai, Johor, Malaysia

<sup>d</sup> Centre for Diploma Studies (CeDS), Universiti Tun Hussein Onn Malaysia, 84600 Muar, Johor, Malaysia

## ARTICLE INFO

### Keywords:

Immobilized titanium dioxide catalyst  
Compounds of emerging concern  
Secondary wastewater effluent  
Non-target screening  
Transformation products

## ABSTRACT

A promising membrane configuration based on immobilized TiO<sub>2</sub> on poly(vinylidene fluoride) (PVDF) dual layer hollow fibre membranes was prepared and successfully employed for the photocatalytic degradation of eight pharmaceuticals. Experiments were carried out in a flow reactor of 0.5 L equipped with a lamp emitting at 254 nm, treating groundwater and secondary wastewater effluent. The efficiency of the new catalyst to photo-transform target micropollutants was demonstrated, being dependent on the selected compound. Only the application of photocatalysis using the supported catalyst allowed to increase the phototransformation rate of trimethoprim, metoprolol and carbamazepine treating secondary wastewater effluent (1.4–2.2 times faster than photolysis). The determination of electrical energy per order of magnitude of transformation (EEO) confirmed the lowest energy requirements to transform selected pharmaceuticals in secondary effluent employing the supported catalyst (33–58 kW h m<sup>-3</sup> compared to 49–79 kW h m<sup>-3</sup> applying only photolysis). The detection and identification of transformation products formed during the investigated treatments was performed by UPLC-QTOF/MS/MS. 156 transformation products were detected showing two different types of time profiles, namely a bell-shape trend or a constant increase along reaction time thus accumulating in the reaction mixture. The chemical structure for 19 out of 156 detected compounds was proposed as derived from parent compounds spiked in the secondary effluent.

## 1. Introduction

A wide variety of factors act as driving forces for the application of post-treatment technologies in wastewater treatment plants (WWTPs) [1]. Increasing demand of fresh water due to the growth of population and the high consumption in agricultural and industrial sectors has promoted the wastewater reuse as a new challenge in water field. Additionally, the risk associated to the presence of compounds of emerging concern (CECs), such as pharmaceutical and personal care products, in secondary effluents due to their incomplete removal during conventional wastewater treatment [2,3] is of public concern taking into account the dangerous effects already demonstrated through different studies [4,5]. Among polishing technologies more applied in WWTPs to obtain effluents exhibiting the necessary requirements for their

posterior destination (either discharge or reuse) are the disinfection technologies [6]. Although different disinfection techniques exist to treat the wastewater, UV treatment is one of the most common technologies applied worldwide in WWTPs due to the competitive advantages that exhibit in comparison to others, such as ozonation or chlorination [7,8]. Even though several studies have demonstrated the potential of UV irradiation to reduce of concentration of pharmaceutical compounds of different nature, such as diclofenac, carbamazepine and trimethoprim, during wastewater treatment, the retention time applied during disinfection step in WWTPs (10–60 s) is not enough to remove efficiently CECs since most of these compounds exhibit slow phototransformation [9–11]. A promising solution to increase the CECs removal efficiency during UV treatment is the combination with catalysts [2,12]. Heterogeneous photocatalysis has become relevant in the

\* Corresponding authors.

E-mail addresses: [marta.carballa@usc.es](mailto:marta.carballa@usc.es) (M. Carballa), [giuseppe.mascolo@ba.irsa.cnr.it](mailto:giuseppe.mascolo@ba.irsa.cnr.it) (G. Mascolo).

last years since chemicals are not necessary for the oxidation processes, being titanium dioxide ( $\text{TiO}_2$ ) the catalyst that is receiving more attention due to the nonspecific nature of the reactive species produced under UV irradiation [13]. During the photocatalytic treatment,  $\text{TiO}_2$  is activated by the UV light generating powerful oxidizing species (e.g. hydroxyl radicals ( $\cdot\text{OH}$ )) which can transform the CECs, even achieving the mineralization of some compounds. However, the application of suspended  $\text{TiO}_2$  is limited at full-scale since the small size of the catalyst complicates its recovery at the end of the treatment, reducing its potential reuse and compromising the quality of treated effluent [14,15]. To overcome this drawback, different authors have studied the immobilization of  $\text{TiO}_2$  particles on different materials, such as polyacrylate, silica and stainless steel [14,16,17]. However, a reduction in the efficiency of the supported catalyst compared to the suspended one due to the decrease of the available active surface is often observed. As a consequence, the development of new catalysts based on  $\text{TiO}_2$  nanosized particles arose as a promising solution to consider the photocatalytic treatment in real applications since nanoparticles exhibit high surface-volume ratio, which increases the density of available active sites for photocatalysis [18–21]. The selection of the support material is a key factor in the fabrication of this type of catalysts since it determines the available area for the dispersion of catalyst nanoparticles, which is directly related to its photoactivity. Different authors have proposed poly(vinylidene fluoride) (PVDF) membrane as a promising support due to the great number of advantages that shows in comparison with other polymeric materials: open structure, thermal stability, mechanical strength, relative chemical inertness and large availability of pore sites (100–500 nm) [22,23]. Moreover, the application of a membrane as a support, especially in dual layer configuration, i.e. pure PVDF in the inner thick layer and composite PVDF/photocatalyst in the outer thin layer, shows the additional advantage of acting as barrier for pollutants and having the photocatalyst supported instead of suspended, improving the quality of treated effluents [24]. However, other kind of membranes designed for the same application are available in the literature [25–29].

The main objective of this study was to assess the application of a promising membrane configuration based on immobilized  $\text{TiO}_2$  on poly(vinylidene fluoride) (PVDF) dual layer hollow fibre membranes [30,31] during photocatalytic treatment of two types of water matrices (groundwater and secondary wastewater effluent), focusing on the elimination of eight selected pharmaceutical compounds. Specifically, the aforementioned co-extruded dual layer membrane with immobilized  $\text{TiO}_2$  was previously synthesized and tested for its filtration and photodegradation performances in removing nonylphenol from synthetic solution, but was not yet employed for the treatment of real groundwater and secondary wastewater effluent. Moreover, a preliminary identification of the transformation products (TPs) formed during photolytic and photocatalytic treatments of secondary wastewater effluent was performed.

## 2. Materials and methods

### 2.1. Selection of pharmaceutical compounds

Eight pharmaceutical compounds not efficiently removed during conventional wastewater treatment and usually detected in secondary wastewater effluents at concentrations in the  $\mu\text{g L}^{-1}$ – $\text{ng L}^{-1}$  range [2,3] were selected as target micropollutants to investigate the removal efficiency of the photocatalytic treatments: carbamazepine (CBZ), diclofenac (DCF), iopromide (IOP), gemfibrozil (GEM), metoprolol (MET), sulfamethoxazole (SMX), trimethoprim (TMP) and warfarin (WAR). Three of them (carbamazepine, diclofenac and metoprolol) are included in Ordinance of Water Protection approved by the Swiss Government [32] which establishes the threshold of reducing their concentration during wastewater treatment by 80% (measured from inlet to outlet of the WWTP). Moreover, diclofenac was included in the

Watch List for the Water Directive Framework through the Decision (EU) 2015/195 but then eliminated in the last revision (Decision (UE) 2018/840) because of the monitoring data available in the year 2017. However, in such a last UE Decision there is no finale conclusion about diclofenac and therefore, the potential risk associated to its presence in the aquatic environment should be monitored in the coming years in order to decide its inclusion or not in the List of Priority Substances [33,34]. All the standard compounds were purchased from Sigma-Aldrich as well as the solvents used for chromatographic analyses and for preparing standard solutions, i.e. acetonitrile, methanol and formic acid (UPLC grade).

A mixed phase photocatalyst titanium dioxide Degussa (Evonik) P25 (mixture of anatase/rutile crystalline phases, surface area  $50 \text{ m}^2/\text{g}$ ) was employed as reference catalyst in photocatalytic experiments [35].

### 2.2. Characterization of groundwater and secondary wastewater effluent

Two water matrices with different complexity in terms of main characteristics (pH, conductivity, volatile and total suspended solids (VSS and TSS), chemical oxygen demand (COD), ammonium ( $\text{N-NH}_4^+$ ), nitrite ( $\text{N-NO}_2^-$ ), nitrate ( $\text{N-NO}_3^-$ ) and total phosphorous (TP)), were employed to evaluate the efficiency of the new catalyst to remove selected pharmaceutical compounds: groundwater and secondary wastewater effluent. Groundwater was collected from a well at a depth of approximately 30 m, whereas secondary wastewater effluent came from a Self-Forming Dynamic Membrane Bioreactor treating municipal wastewater [36]. The physicochemical parameters of both water matrices were determined according to Standard Methods [37] and are listed in Table 1.

### 2.3. Synthesis and characterization of immobilized $\text{TiO}_2$ on the PVDF dual layer hollow fibre membranes

Dual layer hollow fibre (DLHF) membranes were fabricated via a single step co-extrusion technique with immobilized titanium dioxide ( $\text{TiO}_2$ ) nanoparticles embedded in their outer layer, as report elsewhere [30,31]. The DLHF membranes were prepared by extruding through a triple orifice spinneret [38] two different dope solutions simultaneously, in which the inner layer consisted of 18 wt% of poly(vinylidene fluoride) (PVDF) and 82 wt% of solvent *N,N*-dimethylacetamide (DMAc), while the outer layer was a mixture of 15 wt% PVDF, 3 wt%  $\text{TiO}_2$  and 82 wt% DMAc. The spinning procedure and conditions were explained in detail previously [23]. The addition of 3 wt%  $\text{TiO}_2$  nanoparticles at the outer layer in DLHF membranes used in this experiment was based on the optimized performance in term of flux [31] and nonylphenol (NP) photocatalysis degradation [39] in hybrid membrane system.

The details of morphology and properties of the DLHF membranes were analysed by Dzinun et al. [23,30]. The existence of  $\text{TiO}_2$  nanoparticles at the outer layer was proved by scanning electron microscopy (SEM) and energy dispersion X-ray (EDX) analysis as shown in Fig. 1. The DLHF membranes consisted of finger like voids in the inner and

**Table 1**  
Characterization of groundwater and secondary effluent used in this study ( $n = 5$ ).

Parameter	Groundwater	Secondary effluent
pH	$7.7 \pm 0.1$	$7.6 \pm 0.1$
Conductivity ( $\text{mS cm}^{-1}$ )	$2.3 \pm 0.1$	$1.5 \pm 0.1$
TSS ( $\text{mg L}^{-1}$ )	$0.0 \pm 0.0$	$6 \pm 4$
COD ( $\text{mg L}^{-1}$ )	$< 15$	$35 \pm 5$
$\text{N-NH}_4^+$ ( $\text{mg L}^{-1}$ )	$< 1$	$0.4 \pm 0.2$
$\text{N-NO}_3^-$ ( $\text{mg L}^{-1}$ )	$5.5 \pm 0.3$	$40 \pm 4$
$\text{N-NO}_2^-$ ( $\text{mg L}^{-1}$ )	$0.1 \pm 0.0$	$0.3 \pm 0.2$
TP ( $\text{mg L}^{-1}$ )	$< 0.05$	$8 \pm 3$

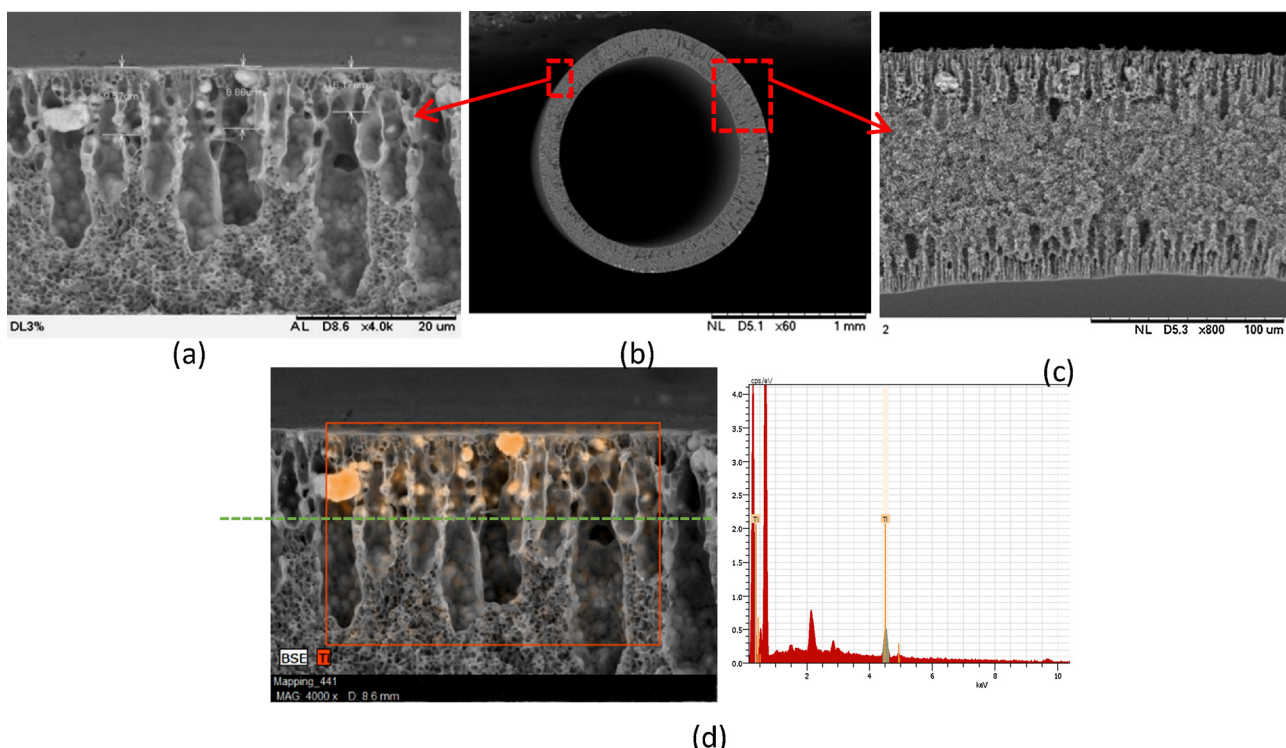


**Fig. 1.** SEM images of the DLHF membranes: (a) outer surface, (b) full cross section, (c) partial cross section, and (d) EDX images of TiO<sub>2</sub> nanoparticles at the outer layer [30].

outer layers, whereas sponge-like structure was formed in between the layers. This structure is called as sandwich-like structure [23]. A seamless interface between the layers was formed due to the good compatibility of both layers and the absence of delamination when the same polymer was used for both inner and outer layer dopes.

The addition of 3 wt% of TiO<sub>2</sub> nanoparticles into the membrane outer layer improves the membrane properties in terms of hydrophilicity, pore size and permeability. The strengthening of OH bonds in the TiO<sub>2</sub> nanoparticles immobilized in DLHF membranes is the main factor in the settlement of TiO<sub>2</sub> nanoparticles on the membrane surface structure [39].

The incorporation of TiO<sub>2</sub> in membrane matrix acts as dual function: on one hand, TiO<sub>2</sub> nanoparticles are activated in the presence of UV light and produce hydroxyl radicals for micropollutants photocatalytic degradation [39], and on the other hand, they reduce membrane fouling [24]. The stability of the dual layer hollow fibre membrane was tested for 30 days under UV exposure in a photocatalytic membrane reactor and the result has been reported by Dzinun et al. [40]. Under this condition, it was found that the DLHF membranes could maintain their integrity, even though many cracks were formed randomly on the irradiated DLHF outer surface and some changes of crystalline phase of PVDF and the formation of –CF=CH– double bond by dehydrofluorination can also be observed.

#### 2.4. Experimental set-up

An up-flow reactor (0.5 L) equipped with a low-pressure mercury UV lamp (40 W) emitting at 254 nm was employed in recirculation mode to carry out the experiments of photolysis and photocatalysis. Two different lamps were used, being the main difference between both lamps the number of hours of operation (< 500 h for lamp 1 and > 1000 h for lamp 2) and, consequently, the fluence rate (50 mW cm<sup>-2</sup> and 41 mW cm<sup>-2</sup>, respectively). A more detailed description of the up-flow reactor can be found in Murgolo et al. [19].

For the photocatalytic experiments using the novel prepared

catalyst, 90 hollow fibres (length: 70 cm) were placed inside the reactor around the quartz tube which protects the UV lamp in order to cover almost its entire length (Fig. S1 of the Supplementary material). An amount of 114 mg of TiO<sub>2</sub> immobilized on the PVDF dual layer hollow fibre membrane was determined, corresponding to a concentration of 57 mg TiO<sub>2</sub> L<sup>-1</sup> (referred to 2 L of solution recirculating through the reactor), which is comparable to 50 mg L<sup>-1</sup> of reference TiO<sub>2</sub> Degussa.

Preliminary tests were performed in order to evaluate the potential adsorption of CECs on the immobilized catalyst, exposing it to a constant up-flow of 6 L water h<sup>-1</sup> during 30 min in darkness.

In addition to the photocatalytic experiments carried out with the novel prepared catalyst, other experiments were performed for comparative purposes: 1) photolysis (only UV irradiation) and 2) conventional heterogeneous photocatalysis using suspended TiO<sub>2</sub> Degussa P25 catalyst (25–300 mg L<sup>-1</sup>). Photolytic and conventional photocatalytic experiments were performed in duplicate whereas photocatalytic tests with the novel supported catalyst were executed on triplicate.

The solutions used during photolytic and photocatalytic experiments were freshly prepared spiking the target pharmaceuticals (concentrations ranging between 200 and 400 µg L<sup>-1</sup>) in groundwater or secondary wastewater effluent, previously filtered through a 0.45 µm pore size filter.

#### 2.5. Analytical techniques

The amount of TiO<sub>2</sub> immobilized in the PVDF membranes was determined by Inductively Coupled Plasma Optical Emission Spectrometry (ICP-OES) preceded by an acid digestion of the solid sample.

The concentration of pharmaceutical compounds in the inlet and outlet of UV system was determined using an Ultimate 3000 System (Thermo Fisher Scientific) equipped with an auto sampler, temperature controlled column compartment and UV detector as a chromatographic system interfaced with a high-resolution mass spectrometer, TripleTOF 5600+ system (AB Sciex) by means of a duo-spray ion source operated

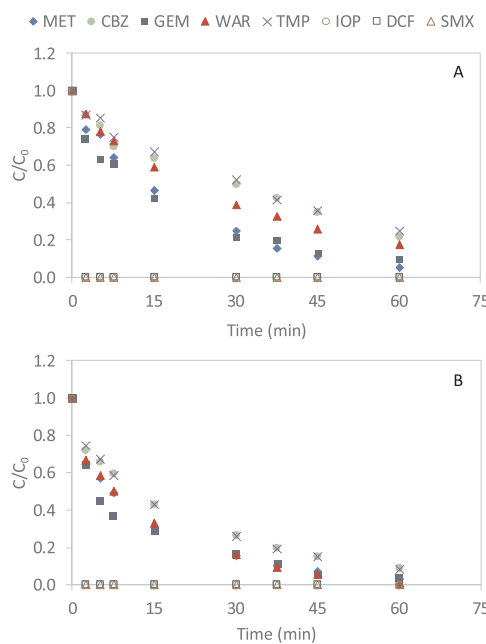


**Fig. 2.** Photolytic transformation of selected pharmaceutical compounds in groundwater (A) and secondary wastewater effluent (B).

in electrospray (ESI) mode (in positive and negative ion modes). All MS analyses were acquired by an information dependent acquisition (IDA) method in high resolution mass spectrometry.

As for the chromatographic separation, a Waters BEH C18 column ( $2.1 \times 150$  mm,  $1.7 \mu\text{m}$ ) is used, operating at a flow of  $0.200 \text{ mL/min}$ .  $20 \mu\text{L}$  samples were injected and eluted with a binary gradient consisting of  $1.5 \text{ mM}$  ammonium acetate in water (A) and  $1.5 \text{ mM}$  ammonium acetate in methanol (B).

The AB Sciex software was used for the quantification, interpretation and processing of data obtained by the high-resolution mass spectrometry analysis while SciexOS 1.2, PeakView 2.2, MasterView 1.1, LibraryView 1.1.0, and MarkerView 3.1 as well as a freely available software, i.e. enviMass 3.4, for non-target screening and trend detection.

#### 2.6. Phototransformation kinetics

The photocatalytic transformation of pharmaceutical compounds follows the Langmuir-Hinshelwood model [Eq. 1], which is used to describe the reactions between the hydroxyl radicals and substrate molecules in either adsorbed or dissolved status [41,42].

$$-\frac{dC}{dt} = \frac{k_t K C}{1 + KC} \quad (1)$$

where  $k_t$  is the rate constant affected by different parameters, such as the mass of catalyst, the flux of efficient photons and the coverage in oxygen [17],  $K$  is the adsorption coefficient of the substance to be transformed and  $C$  is its concentration.

Since the initial concentration of pharmaceutical compounds is very low (in the order of  $\mu\text{g L}^{-1}$ ), the equation Eq. (1) can be simplified to a pseudo first order kinetics Eq. (2)

$$\ln(C/C_0) = -k_t K t = -k t \quad (2)$$

where  $k$  is the apparent rate constant of the pseudo first order reaction,  $t$  is the time of treatment and  $C/C_0$  the ratio between the final and initial concentrations of pharmaceuticals.

#### 2.7. Electrical energy per order of transformation

The energy efficiency of UV-based advanced oxidation processes is

usually expressed in terms of electrical energy per order of transformation (EEO) since the operating cost is mainly associated to electrical consumption. EEO is defined as the number of kWh of electrical energy required to reduce the concentration of a pollutant by one order of magnitude in  $1 \text{ m}^3$  of contaminated water [19,43], and was determined employing the following equation:

$$EEO = \frac{P_{UV}}{Q \cdot \ln(C_0/C)} \quad (3)$$

where  $P_{UV}$  is the power of UV lamp ( $\text{kW}$ ),  $Q$  is the flow of treated water ( $\text{m}^3 \text{ h}^{-1}$ ) and  $C_0$  and  $C$  are the initial and final concentrations of each substance ( $\mu\text{g L}^{-1}$ ).

#### 2.8. Non-target screening and transformation products identification

All the collected IDA-MS data files, corresponding to the different reaction times for a specific treatment, were processed for non-target screening using a data workflow in enviMass 3.4 software [44]. Briefly, the approach used for the interpretation and processing of data is as follows: an initial peak picking by enviMass generates a list of ions with a corresponding retention time and peak intensity in each acquired file. The list of ions is subsequently reduced by intersection of replicate samples, removal of peaks which have also been detected in blank samples, isotope grouping and adduct grouping. The obtained peak lists were then processed in SciexOS software for detecting significant trends as well as for identification of unknown compound, employing both the formula finder based on isotopic pattern and library searching capabilities (LibraryView). Structure identification was then attempted based on high resolution MS-MS data [45]. Moreover, linking these results to ChemSpider, a more confident identification of detected compounds in investigated samples was performed. The peaks for which a typical trend of transformation products was identified were further processed by R statistical environment, using a linkage analysis script, in order to obtain further information about the structure of the metabolite. Finally, the peak lists were also employed for the principal component analysis (PCA) using the MarkerView 3.1 software.

### 3. Results and discussion

#### 3.1. Photolysis of pharmaceuticals: groundwater vs. secondary effluent

The efficiency of UV treatment to reduce the concentration of selected pharmaceutical substances was demonstrated using both groundwater and secondary wastewater effluent (Fig. 2). The obtained results evidenced that phototransformation rate depends directly on both the type of the organic pollutant and the type of water matrix. DCF, SMX and IOP were rapidly phototransformed (2.5 min was enough to observe their complete disappearance) regardless the water matrix, while the phototransformation of the rest of compounds was lower, being TMP and CBZ the compounds that exhibited slower kinetics. This observation is consistent with previous works [10,46], which confirmed that the phototransformation is compound-dependent since the chemical structure of the compounds plays an important role on the efficiency of direct photolysis. In fact, Afonso-Olivares et al. [47] had already classified DCF and SMX as compounds highly prone to be phototransformed under direct UV employing a low-pressure UV lamp, whereas TMP and CBZ were grouped together because of their slow phototransformation.

The influence of the water matrix was only observed for the compounds that exhibited slow phototransformation rate (WAR, TMP, MET, CBZ and GEM), being the obtained kinetic constants always slightly higher testing secondary effluent ( $0.04\text{--}0.06 \text{ min}^{-1}$  compared to  $0.02\text{--}0.05 \text{ min}^{-1}$  for groundwater) (Figs. 3 and S2). Although a priori groundwater is expected to be a better candidate for photolytic treatment than secondary wastewater effluent since it exhibits a less

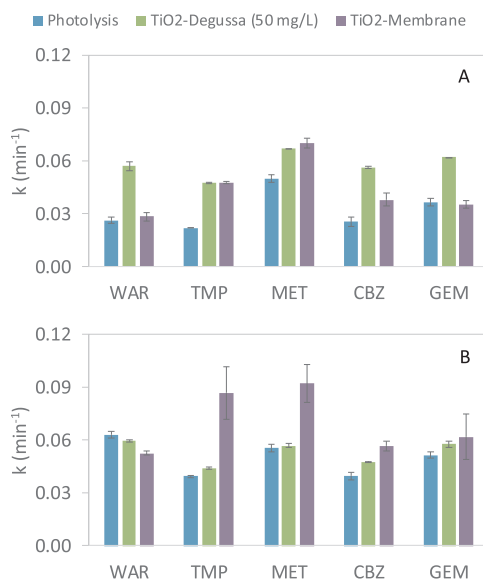


**Fig. 3.** Photocatalytic performance of TiO<sub>2</sub>-membrane catalyst compared to photolysis and conventional photocatalysis for the removal of selected CECs treating groundwater (A) and secondary wastewater effluent (B).

complex matrix (Table 1), the results evidenced that the composition of the secondary wastewater effluent enhances the efficiency of UV treatment. The reason is that different reactions can take place between the UV light and some compounds present in the secondary effluent, such as nitrate or dissolved organic matter, which can favour the formation of hydroxyl radicals, thus increasing the efficiency of the photolysis [48,49]. In this study, the better results obtained with secondary effluent are probably due to a combined effect of the secondary effluent matrix, and specially of the nitrate (Table 1), since the production of hydroxyl radicals from nitrate during the photolytic treatment of wastewater is widely demonstrated in literature [11,48].

### 3.2. Photocatalytic transformation of target compounds

The results obtained from the preliminary adsorption tests (Fig. S3) demonstrated that the adsorption of selected pharmaceuticals on the surface of both suspended (TiO<sub>2</sub> Degussa P25) and supported (TiO<sub>2</sub>-membrane) catalysts was negligible (< 10%). These adsorption percentages are comparable to those observed in literature for other catalysts (for instance, immobilized TiO<sub>2</sub> nanoparticles on commercial hollow fibre membranes, Fe<sub>3</sub>O<sub>4</sub>/SiO<sub>2</sub>/TiO<sub>2</sub> particles or TiO<sub>2</sub>/zeolite composites) used in the photocatalytic treatment of pharmaceutical compounds in wastewater [29,50,51]. Consequently, the differences observed between the photolytic and photocatalytic processes for each compound (Fig. 3) are only associated to the activation of the TiO<sub>2</sub> particles by UV light. Taking in account this fact, the main mechanism involved in the photocatalytic transformation of selected pharmaceutical compounds is attributed to the oxidation of the organic micro-pollutants through the reaction with hydroxyl radicals. These radicals are produced by the reaction between the hole created in the valence band ( $h^+$ ) and the water molecules or the hydroxyl ions adsorbed on the surface of catalyst particles, when the particles of TiO<sub>2</sub> are irradiated with UV light [52].

The positive effect of photocatalysis was only identified for five out of eight selected pharmaceutical compounds since diclofenac, iopromide and sulfamethoxazole were so fast eliminated during photolysis that was not possible to determine the influence of the catalyst under the experimental conditions of this study. For these five pharmaceuticals, the photocatalytic transformation follows a pseudo-first order kinetics employing both groundwater and secondary wastewater effluent. The kinetic constants obtained for each CEC during photolysis

and photocatalysis (employing both immobilized TiO<sub>2</sub> on PVDF membrane and suspended TiO<sub>2</sub> Degussa P25 catalyst) using groundwater and secondary effluent, are summarized in Fig. 3.

During the experiments carried out with groundwater (Fig. 3A), the application of the supported catalyst allowed to increase the photo-transformation rate of trimethoprim, carbamazepine and metoprolol compared to the photolytic reaction (k was between 1.4 and 2.2 times faster), whereas the kinetic constants obtained for warfarin and gemfibrozil were in the same range (0.026 and 0.035 min<sup>-1</sup>, respectively). Compared to the suspended TiO<sub>2</sub> catalyst, the supported catalyst showed a similar efficiency to eliminate trimethoprim and metoprolol, whereas the efficiency was lower for carbamazepine (0.04 vs 0.06 min<sup>-1</sup>). Although the employment of the suspended catalyst was highly effective since it allowed to increase the removal of the five target compounds with respect to photolysis (k was between 1.3 and 2.2 times faster than using only UV irradiation), also observing an increase in the efficiency of the suspended catalysts when the concentration of Degussa P25 was increased from 25 to 300 mg L<sup>-1</sup> (Table S1), the limitation in the recovery of the catalyst compromises its use since a significant fraction remained stuck on the walls of the reactor, being not recoverable. In addition, a centrifugation step was necessary to separate the catalyst from the treated water.

It is known that the efficiency of photocatalysis is compound-dependent since some functional groups show higher susceptibility to be degraded than others during the photocatalytic treatment induced by TiO<sub>2</sub> (e.g. aldehydes and ketones versus aromatic cyclic compounds) [53]. In addition, the differences observed using suspended and supported catalysts could be attributed to other factors, such as the individual contribution of the mechanisms involved in the photocatalytic transformation of the pollutants [53,54]. While the oxidative reaction between the pollutant and dissolved hydroxyl radicals (generated on TiO<sub>2</sub> surface and subsequently desorbed) is only slightly affected by the chemical structure of the compound, the mechanism based on the direct reaction between the pollutant adsorbed on the surface of semiconductor and the hole created in the valence band when UV light falls upon TiO<sub>2</sub> particles depends strongly on the pollutant molecule since its chemical structure (functional groups, charge and size) determines its adsorption on TiO<sub>2</sub> surface [55].

During the experiments carried out with secondary wastewater effluent (Fig. 3B), the efficiency of the supported TiO<sub>2</sub>-membrane catalyst compared to photolysis was also demonstrated for the same three compounds already affected using groundwater (trimethoprim, metoprolol and carbamazepine). Surprisingly, contrarily to the behaviour observed during the experiments using groundwater, the efficiency of conventional suspended catalyst was quite low since the kinetic constants obtained were very similar to those determined using only photolysis, regardless the concentration of suspended catalyst applied (50 or 100 mg L<sup>-1</sup>) (Table S2). Metoprolol and trimethoprim exhibited the highest kinetic constants ( $k > 0.08 \text{ min}^{-1}$ ), much higher than those obtained employing the conventional suspended TiO<sub>2</sub> Degussa catalyst ( $k < 0.05 \text{ min}^{-1}$ ), while for carbamazepine, the differences were lower ( $k > 0.06 \text{ min}^{-1}$  vs.  $k$  around  $0.04 \text{ min}^{-1}$ ). In contrast, warfarin was more vulnerable to photolysis than to photocatalysis employing the supported catalyst (Fig. 3B), which suggests that a shadow effect could be exerted by the catalyst, hindering that UV light could directly attack the molecules of warfarin. Although the matrix effect was observed for both catalysts, the supported catalyst showed high efficiency to phototransform metoprolol, carbamazepine and trimethoprim, regardless the type of matrix, whereas the efficiency of the suspended catalyst was more affected by the water composition being strongly reduced during the treatment of secondary effluent. This behaviour observed for the suspended TiO<sub>2</sub> Degussa catalyst is in accordance with previous studies which demonstrated the inhibitory effect on the photocatalytic activity of TiO<sub>2</sub> of some compounds detected in high concentration in treated wastewater matrices, such as dissolved organic matter and nitrate [56,57]. Choi et al. [12] observed a significant reduction in the

phototransformation rate of pharmaceutical compounds during the photocatalytic treatment of secondary effluents which exhibited high concentration of dissolved organic carbon. This finding was attributed to the competition between both pollutants for the surface-active sites of TiO<sub>2</sub> Degussa P25 and the hydroxyl radicals generated. Also nitrate might have an effect, despite literature is not consistent. Friedmann et al. [55] and Umar and Aziz [57] identified the inhibitory effect of nitrate in photocatalytic reactions since this compound can be adsorbed on the surface of TiO<sub>2</sub> blocking the active sites, but Choi et al. [12] did not observe a clear impact on the phototransformation of carbamazepine.

In order to get insights about the effectiveness of the photocatalytic process with supported TiO<sub>2</sub>, other organic pollutants were searched in the secondary wastewater effluent and their fate monitored during the tested treatments. The analytical screening procedure (described in Section 2.8) allowed detecting 86 compounds in the secondary effluent. For some of the detected compounds it was possible to attribute a pharmaceutical compound confidently, for some others, it was only possible to propose an elemental composition, and for the remaining, no chemical information could be elucidated because the intensity of their MS signal was quite low (Table S3). For all the detected compounds, it was possible to measure the pseudo-first order kinetic constant during the three UV-based treatments (Table S3), with the exception of those compounds disappearing too fast during the reactions (23.3% of the detected compounds). TiO<sub>2</sub>-membrane and the suspended TiO<sub>2</sub> catalysts showed a faster decay for 23.3% and for 38.4% of the compounds, respectively. For the remaining 15.1% of compounds, the three treatments gave similar degradation rates. Overall, when taking into account a big number of compounds to be compared for degradation rates by the investigated UV-based processes, results showed that the TiO<sub>2</sub>-membrane performed quite efficiently (Fig. 4). The latter combined with the benefit of having the catalyst supported onto the membrane, thus avoiding a further treatment step for the recovery of the TiO<sub>2</sub> powder as for the conventional Degussa catalyst, promotes the use of immobilized catalyst for secondary effluents post-treatment.

The efficiency of the supported catalyst was evaluated during five reaction cycles (Table S4) and the results obtained showed that it can be reused several times without reducing its capacity to phototransform selected pharmaceutical compounds, confirming the advantage about

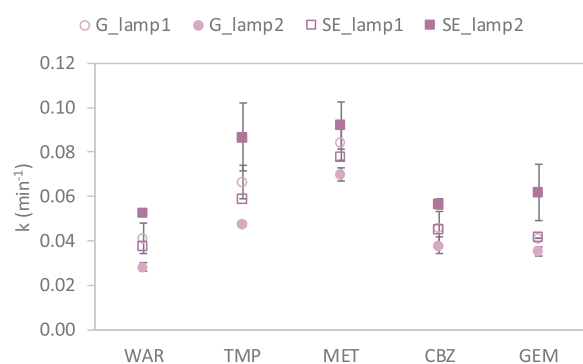


**Fig. 5.** Photocatalytic transformation of target pharmaceuticals in groundwater (G) and secondary effluent (SE) using immobilized TiO<sub>2</sub> on PVDF dual-layer membranes and lamps 1 and 2 (operation time: < 500 h and > 1000 h, respectively).

the application of supported compared to suspended catalysts.

### 3.3. Influence of lamp irradiance on the efficiency of supported catalyst

With the purpose of evaluating the influence of lamp irradiance on the efficiency of the novel supported catalyst, two UV lamps of 40 W emitting at 254 nm were employed, being the main difference between them the number of hours of operation (< 500 h for lamp 1 and > 1000 h for lamp 2). Based on the results obtained treating groundwater and secondary effluent (Fig. 5), it can be observed that the photo-sensitivity of selected CECs was not influenced by the lamp used since trimethoprim and metoprolol were the fastest phototransformed compounds compared to carbamazepine, gemfibrozil and warfarin. However, the phototransformation rate of each compound was affected by the lamp employed since the photon flux emitted is function of the number of hours of operation [58]. As expected, since the photon flux emitted by the lamp 1 was slightly higher because it had been operated during less hours (< 500 h), higher photocatalytic constants were obtained during the experiments performed with lamp 1 treating groundwater (between 1.2 and 1.5 times faster than those obtained with lamp 2). Nevertheless, the experiments carried out with secondary effluent demonstrated that, still using the lamp 2 which emitted lower

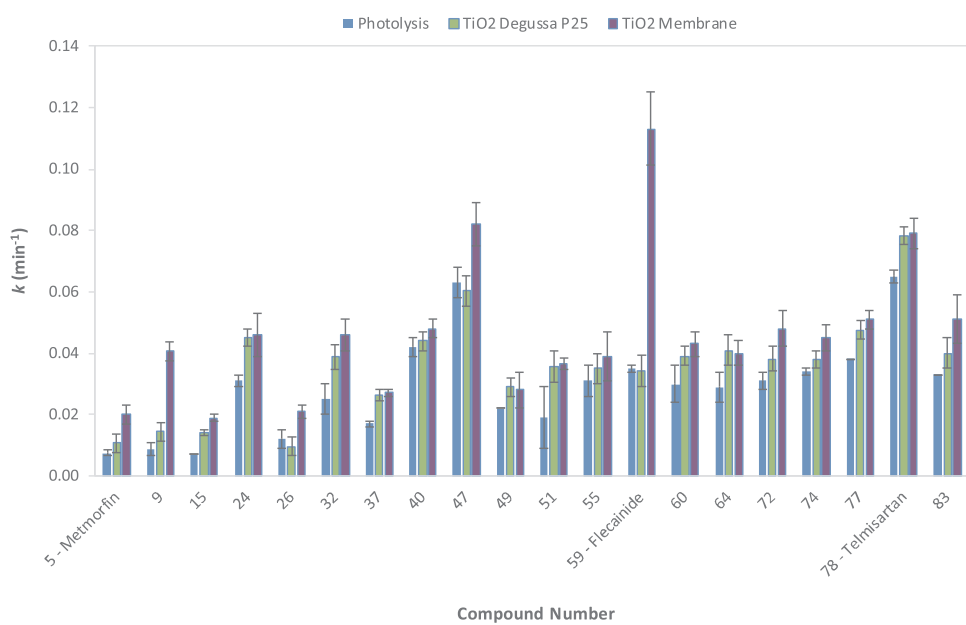


**Fig. 4.** Photocatalytic performance of TiO<sub>2</sub>-membrane catalyst as compared to photolysis and conventional photocatalysis for the removal of identified suspect compounds naturally present in the investigated secondary wastewater effluent.

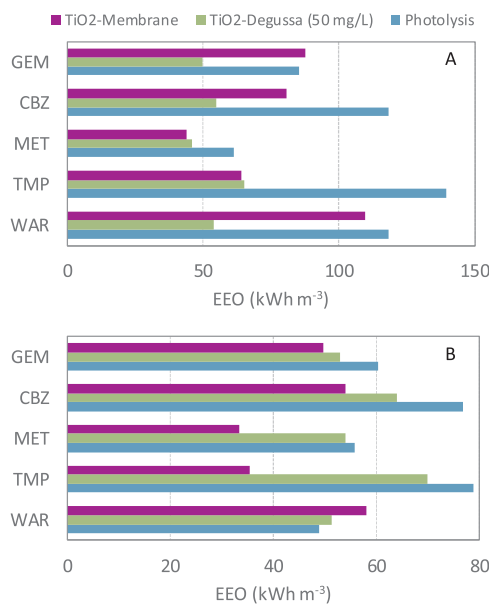


**Fig. 6.** Electrical energy per order of transformation of selected CECs corresponding to photolysis and photocatalysis treating both groundwater (A) and secondary effluent (B).

photon flux (according to American Air&Water [58]), it was possible to obtain similar or even higher (up to 1.5 times faster) photocatalytic constants than applying the lamp 1. This fact could be explained considering that the lower photon flux of the lamp can be compensated by other factors, such as water composition, which have strong influence on photocatalytic treatment. Although in general the characterization of secondary effluent was similar during the different experiments (Table 1), slight differences were detected in terms of nitrate concentration (around 35 and 44 mg N-NO<sub>3</sub> L<sup>-1</sup> during the experiments using lamp 1 and lamp 2, respectively). Consequently, the concentration of nitrate might have a positive influence on the efficiency of immobilized TiO<sub>2</sub> on PVDF membrane catalyst using lamp 2, promoting its potential application in the post-treatment of treated wastewater

effluents.

### 3.4. Energy requirement for the removal of CECs

**Fig. 6** summarizes the EEO values obtained for photolysis and photocatalysis treating both groundwater and secondary wastewater effluent. As expected, the electrical consumption depends on the water quality and varies in function of selected pharmaceutical since the efficiency of photolytic and photocatalytic treatments are compound-specific. In general, the application of photocatalysis reduced the electrical requirements to phototransform selected CECs in comparison to only photolysis. While EEO between 44 and 110 kWh m<sup>-3</sup> were necessary to transform target pharmaceutical compounds in groundwater employing immobilized TiO<sub>2</sub> on PVDF dual layer hollow fibre membrane (61–140 kWh m<sup>-3</sup> for photolysis), lower electrical requirements (33–58 kWh m<sup>-3</sup>) were demanded for secondary effluent (49–79 kWh m<sup>-3</sup> for photolysis) due to the photosensitizer effect of the water matrix. Thus, the EEO was reduced from around 30% for metoprolol to 55% for trimethoprim using the supported catalyst. When suspended TiO<sub>2</sub> (Degussa P25) and immobilized TiO<sub>2</sub> on PVDF membrane were compared from the energetic consumption point of view, the use of the supported catalyst to treat secondary effluent was again justified since lower EEO values were obtained (**Fig. 6**).

### 3.5. Identification of phototransformation products

The analytical protocol employed for the non-target organics screening also allowed to detect compounds not present in the secondary effluent at the beginning of the UV-based experiments that could be thus confidently associated to TPs. By a careful investigation of the detected compounds, 156 metabolites were rationally identified (Table S5). All the TPs showed to follow two different types of time profiles, namely a bell-shape trend or a constant increase along reaction time, thus accumulating in the reaction mixture. For 19 out of 156 detected TPs, a chemical structure was proposed and derived from the parent CEC spiked in the secondary wastewater effluent, namely from carbamazepine (5 TPs), metoprolol (6 TPs), gemfibrozil (2 TPs), trimethoprim (4 TPs), warfarin (2 TPs), as listed in Table S6. No degradation products of diclofenac, sulfamethoxazole and iopromide were

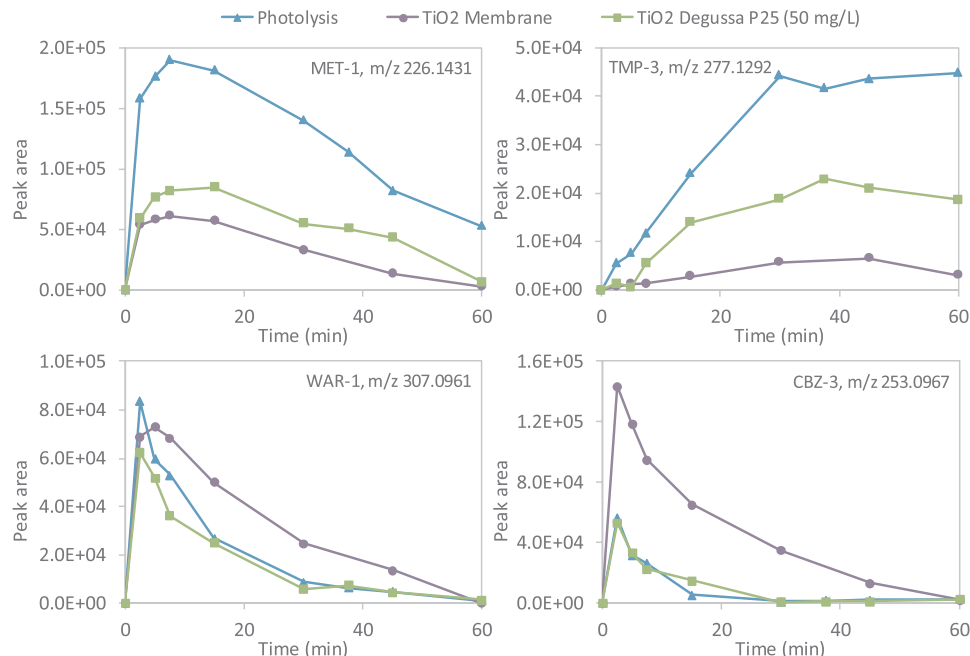


**Fig. 7.** Time profiles of the transformation products MET-1, TMP-3, WAR-1 and CBZ-3 during photolysis, photocatalysis with suspended TiO<sub>2</sub> (Degussa P25) and photocatalysis with immobilized TiO<sub>2</sub> on PVDF membranes, using secondary wastewater effluent.

identified. It is worth noting that for 5 out of 19 TPs listed in Table S6, the proposed chemical structures matched those present in the Metlin MS/MS database [59].

The most representative profiles of identified TPs are shown in Fig. 7, which were obtained by plotting the peak area of the selected metabolites along reaction time. Overall, four different trends were found: (i) the photolytic treatment generates a TP with higher intensity respect to both photocatalytic treatments, with a subsequently lower removal extend of the compound (MET-1); (ii) the TP production increases with time of the treatment (especially during photolytic treatment), and no further degradation (TMP-3); (iii) no relevant differences are observed between the three treatments since the TP is accumulated and subsequently removed in the same extension (WAR-1); and finally, (iv) a higher accumulation of the TP is observed during the first minutes of photocatalytic treatment using supported catalyst, but similar global removal is achieved applying the three treatments (CBZ-3). It is worth noting that the non-target screening could be enlarged by extending the polarity of detectable organics with other chromatographic columns [60].

The principal component analysis (PCA) was conveniently applied to all the detected compounds, namely employing as an input list both the spiked and detected compounds in the secondary effluent and all detected TPs, for an overall comparison of the three UV-based treatments. As PCA attempts to explain as much variation as possible in as few components as possible, it results a useful tool to describe the three different investigated reactions at several reaction time and has been already employed for comparing different wastewater treatments [61]. Conversely, the conventional comparison based on compounds present both at each investigated reaction and at each reaction time would be unpractical considering the high number of compounds present (including both the spiked compounds, the 86 detected compounds and the 156 TPs) and the different intensity of each compound. The result of the PCA is the generation of new variables ranked by accounting the largest difference between the samples. Therefore, a score plot can be obtained by plotting the score assigned to each sample for first two variables (Fig. 8) where the first principal component variable (D1), explaining 21.2% of variance, can be attributed to the difference in sample type (i.e. initial sample vs treated sample). D2 (plotted along the y-axis), also explaining 21.2% of variance, can be attributed to the differences in reaction time and in the different performed treatment.

Results (Fig. 8) show that after 7.5 min of reaction, samples were already quite different from the initial secondary effluent sample (0 min) especially along the principal component D1. Moreover, it is interesting the behaviour of the samples arising from photocatalysis with suspended TiO<sub>2</sub> along the reaction time. At 7.5 min, the sample is located closer to the replicates of photocatalysis with TiO<sub>2</sub>-membrane than to the replicates of photolysis, suggesting that all the samples arising photocatalytic reactions are quite different from those arising from photolysis (Fig. 8). Instead, the samples at 15 min and 60 min of reaction time are clearly much closer to the photolysis replicate samples. This finding is consistent with the fact that at longer reaction time, the composition of the TiO<sub>2</sub>-membrane photocatalysis sample resulted to be quite different from the TiO<sub>2</sub>-suspended photocatalysis sample in terms of residual abundance of both the parent compounds and the TPs. Indeed, this can be associated to the better performance of the TiO<sub>2</sub>-membrane photocatalysis in terms of faster degradation of the 86 detected compounds being the number of detected TPs and their minimization similar for the TiO<sub>2</sub>-membrane photocatalysis and the TiO<sub>2</sub>-suspended photocatalysis processes.

#### 4. Conclusions

The application of a novel catalyst based on immobilized TiO<sub>2</sub> on PVDF dual-layer hollow fibre membranes for the phototransformation of eight target pharmaceuticals was evaluated, comparing its efficiency during the treatment of groundwater and a secondary wastewater effluent. Carbamazepine, trimethoprim and metoprolol were more rapidly phototransformed compared to only photolysis, regardless the water matrix. In contrast to the conventional suspended catalyst, the application of the supported catalyst allowed to increase the phototransformation rate of these compounds during the photocatalytic treatment of the secondary effluent. It was demonstrated that the supported catalyst can be easily reused without losing efficiency and avoiding the need of additional separation systems (e.g. membranes) to recover it. The fate of 156 metabolites formed during the photolytic and photocatalytic treatments was assessed, observing a lower accumulation for most of them during the first minutes of photocatalytic treatment. Although further research is needed to demonstrate the versatility of the novel catalyst and its potential to be reused during a long period of time, its application emerges as a promising option to

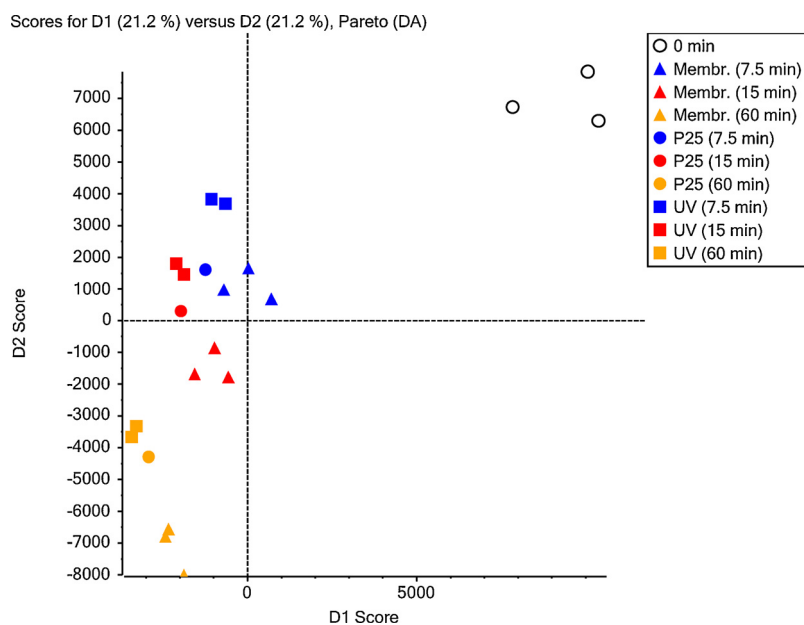


**Fig. 8.** Score plots obtained from PCA when employed to the spiked compounds, the detected compounds (Table S3) and the transformation products detected by non-target organics screening (Table S5) in photolytic and photocatalytic experiments (TiO<sub>2</sub> membrane and TiO<sub>2</sub> Degussa P25) with secondary wastewater effluent.

upgrade UV systems in WWTPs to maximize CECs elimination.

## Acknowledgments

This Special Issue is dedicated to honor the retirement of Dr. John Kiwi at the Swiss Federal Institute of Technology (Lausanne), a key figure in the topic of photocatalytic materials for the degradation of contaminants of environmental concern. This work was conceived within a Short Term Scientific Mission funded by COST Action ES1205 “ENTER-The transfer of engineered nanomaterials from wastewater treatment & stormwater to rivers”. Authors from Universidade de Santiago de Compostela belong to the Galician Competitive Research Group GRC ED431C2017/29 and to the CRETUS Strategic Partnership (AGRUP2015/02). Both programmes are co-funded by FEDER (EU). Authors also want to thank Pompilio Vergine, Carlo Salerno and Giovanni Berardi for their support in the data provision about secondary wastewater effluent. This work was partially supported by the EC-funded 7th FP Project LIMPID (Grant No. 310177).

## Appendix A. Supplementary data

Supplementary material related to this article can be found, in the online version, at doi:<https://doi.org/10.1016/j.apcatb.2018.08.067>.

## References

- [1] W.U.N.W.W.A. Programme, Wastewater: the untapped resource, The United Nations World Water Development Report 2017, UNESCO, Paris, 2017.
- [2] Y. Luo, W. Guo, H.H. Ngo, L.D. Nghiem, F.I. Hai, J. Zhang, S. Liang, X.C. Wang, A review on the occurrence of micropollutants in the aquatic environment and their fate and removal during wastewater treatment, *Sci. Total Environ.* 473–474 (2014) 619–641.
- [3] N.H. Tran, M. Reinhard, K.Y.-H. Gin, Occurrence and fate of emerging contaminants in municipal wastewater treatment plants from different geographical regions—a review, *Water Res.* 133 (2018) 182–207.
- [4] L. Rizzo, C. Manaia, C. Merlin, T. Schwartz, C. Dagot, M.C. Ploy, I. Michael, D. Fatta-Kassinos, Urban wastewater treatment plants as hotspots for antibiotic resistant bacteria and genes spread into the environment: a review, *Sci. Total Environ.* 447 (2013) 345–360.
- [5] A.R. Schwindt, D.L. Winkelmann, K. Keteles, M. Murphy, A.M. Vajda, An environmental oestrogen disrupts fish population dynamics through direct and transgenerational effects on survival and fecundity, *J. Appl. Ecol.* 51 (2014) 582–591.
- [6] European Environment Agency (EEA), Urban Wastewater Treatment, European Environment Agency, Copenhagen, 2017 pp. 22.
- [7] T. Rudd, L.M. Hopkinson, Comparison of disinfection techniques for sewage and sewage effluents, *Water Environ. J.* 3 (1989) 612–618.
- [8] V. Mezzanotte, M. Antonelli, S. Citterio, C. Nurizzo, Wastewater disinfection alternatives: chlorine, ozone, peracetic acid, and UV light, *Water Environ. Res.* 79 (2007) 7.
- [9] N. Collado, S. Rodriguez-Mozaz, M. Gros, A. Rubirola, D. Barceló, J. Comas, I. Rodriguez-Roda, G. Buttiglieri, Pharmaceuticals occurrence in a WWTP with significant industrial contribution and its input into the river system, *Environ. Pollut.* 185 (2014) 202–212.
- [10] J.C. Carlson, M.I. Stefan, J.M. Parnis, C.D. Metcalfe, Direct UV photolysis of selected pharmaceuticals, personal care products and endocrine disruptors in aqueous solution, *Water Res.* 84 (2015) 350–361.
- [11] L. Paredes, F. Omil, J.M. Lema, M. Carballa, What happens with organic micropollutants during UV disinfection in WWTPs? A global perspective from laboratory to full-scale, *J. Hazard. Mater.* 342 (2018) 670–678.
- [12] J. Choi, H. Lee, Y. Choi, S. Kim, S. Lee, S. Lee, W. Choi, J. Lee, Heterogeneous photocatalytic treatment of pharmaceutical micropollutants: effects of wastewater effluent matrix and catalyst modifications, *Appl. Catal. B* 147 (2014) 8–16.
- [13] M.J. Arlos, M.M. Hatat-Fraile, R. Liang, L.M. Bragg, N.Y. Zhou, S.A. Andrews, M.R. Servos, Photocatalytic decomposition of organic micropollutants using immobilized TiO<sub>2</sub> having different isoelectric points, *Water Res.* 101 (2016) 351–361.
- [14] M. Borges, D. García, T. Hernández, J. Ruiz-Morales, P. Esparza, Supported photocatalyst for removal of emerging contaminants from wastewater in a continuous packed-bed photoreactor configuration, *Catalysts* 5 (2015) 77.
- [15] C. Byrne, G. Subramanian, S.C. Pillai, Recent advances in photocatalysis for environmental applications, *J. Environ. Chem. Eng.* 6 (2018) 3531–3555.
- [16] R. Comparelli, P.D. Cozzoli, M.L. Curri, A. Agostiano, G. Mascolo, G. Lovecchio, Photocatalytic degradation of methyl-red by immobilised nanoparticles of TiO<sub>2</sub> and ZnO, *Water Sci. Technol.* 49 (2004) 183–188.
- [17] A. Fernández, G. Lassaletta, V.M. Jiménez, A. Justo, A.R. González-Elipe, J.M. Herrmann, H. Tahiri, Y. Ait-Ichou, Preparation and characterization of TiO<sub>2</sub> photocatalysts supported on various rigid supports (glass, quartz and stainless steel). Comparative studies of photocatalytic activity in water purification, *Appl. Catal. B* 7 (1995) 49–63.
- [18] S. Murgolo, F. Petronella, R. Ciannarella, R. Comparelli, A. Agostiano, M.L. Curri, G. Mascolo, UV and solar-based photocatalytic degradation of organic pollutants by nano-sized TiO<sub>2</sub> grown on carbon nanotubes, *Catal. Today Part A* 240 (2015) 114–124.
- [19] S. Murgolo, V. Yargeau, R. Gerbasi, F. Visentin, N. El Habra, G. Ricco, I. Lacchetti, M. Carere, M.L. Curri, G. Mascolo, A new supported TiO<sub>2</sub> film deposited on stainless steel for the photocatalytic degradation of contaminants of emerging concern, *Chem. Eng. J.* 318 (2017) 103–111.
- [20] B. Srikanth, R. Goutham, R. Badri Narayan, A. Ramprasad, K.P. Gopinath, A.R. Sankaranarayanan, Recent advancements in supporting materials for immobilised photocatalytic applications in waste water treatment, *J. Environ. Manage.* 200 (2017) 60–78.
- [21] F. Petronella, E. Fanizza, G. Mascolo, V. Locaputo, L. Bertinetti, G. Martra, S. Coluccia, A. Agostiano, M.L. Curri, R. Comparelli, Photocatalytic activity of nanocomposite catalyst films based on nanocrystalline metal/semiconductors, *J. Phys. Chem. C* 115 (2011) 12033–12040.
- [22] S.S. Chin, K. Chiang, A.G. Fane, The stability of polymeric membranes in a TiO<sub>2</sub> photocatalysis process, *J. Membr. Sci.* 275 (2006) 202–211.
- [23] H. Dzinun, M.H.D. Othman, A.F. Ismail, M.H. Puteh, M.A. Rahman, J. Jaafar, Morphological study of co-extruded dual-layer hollow fiber membranes incorporated with different TiO<sub>2</sub> loadings, *J. Membr. Sci.* 479 (2015) 123–131.
- [24] H. Dzinun, M.H.D. Othman, A.F. Ismail, M.H. Puteh, M.A. Rahman, J. Jaafar, Stability study of PVDF/TiO<sub>2</sub> dual layer hollow fibre membranes under long-term UV irradiation exposure, *J. Water Process. Eng.* 15 (2017) 78–82.
- [25] L. Aoudjit, P.M. Martins, F. Madjene, D.Y. Petrovych, S. Lanceros-Mendez, Photocatalytic reusable membranes for the effective degradation of tartrazine with a solar photoreactor, *J. Hazard. Mater.* 344 (2018) 408–416.
- [26] S. Teixeira, P.M. Martins, S. Lanceros-Méndez, K. Kühn, G. Cuniberti, Reusability of photocatalytic TiO<sub>2</sub> and ZnO nanoparticles immobilized in poly(vinylidene difluoroide)-co-trifluoroethylene, *Appl. Surf. Sci.* 384 (2016) 497–504.
- [27] N.A. Almeida, P.M. Martins, S. Teixeira, J.A. Lopes da Silva, V. Sencadas, K. Kühn, G. Cuniberti, S. Lanceros-Mendez, P.A.A.P. Marques, TiO<sub>2</sub>/graphene oxide immobilized in P(VDF-TrFE) electrospun membranes with enhanced visible-light-induced photocatalytic performance, *J. Mater. Sci.* 51 (2016) 6974–6986.
- [28] P.M. Martins, R. Miranda, J. Marques, C.J. Tavares, G. Botelho, S. Lanceros-Mendez, Comparative efficiency of TiO<sub>2</sub> nanoparticles in suspension vs. immobilization into P(VDF-TrFE) porous membranes, *RSC Adv.* 6 (2016) 12708–12716.
- [29] S. Teixeira, H. Mora, L.-M. Blasse, P.M. Martins, S.A.C. Carabineiro, S. Lanceros-Méndez, K. Kühn, G. Cuniberti, Photocatalytic degradation of recalcitrant micropollutants by reusable Fe<sub>3</sub>O<sub>4</sub>/SiO<sub>2</sub>/TiO<sub>2</sub> particles, *J. Photochem. Photobiol. A Chem.* 345 (2017) 27–35.
- [30] H. Dzinun, M.H.D. Othman, A.F. Ismail, M.H. Puteh, M.A. Rahman, J. Jaafar, Performance evaluation of co-extruded microporous dual-layer hollow fiber membranes using a hybrid membrane photoreactor, *Desalination* 403 (2017) 46–52.
- [31] H. Dzinun, M.H.D. Othman, A.F. Ismail, M.H. Puteh, M.A. Rahman, J. Jaafar, N. Adrus, N.A. Hashim, Antifouling behavior and separation performance of immobilized TiO<sub>2</sub> in dual layer hollow fiber membranes, *Polym. Eng. Sci.* (2018), <https://doi.org/10.1002/pen.24753> in press.
- [32] I. Logar, R. Brouwer, M. Maurer, C. Ort, Cost-benefit analysis of the swiss national policy on reducing micropollutants in treated wastewater, *Environ. Sci. Technol.* 48 (2014) 12500–12508.
- [33] J.C.G. Sousa, A.R. Ribeiro, M.O. Barbosa, M.F.R. Pereira, A.M.T. Silva, A review on environmental monitoring of water organic pollutants identified by EU guidelines, *J. Hazard. Mater.* 344 (2018) 146–162.
- [34] P. Schröder, B. Helmreich, B. Škrbić, M. Carballa, M. Papa, C. Pastore, Z. Emre, A. Oehmen, A. Langenhoff, M. Molinos, J. Dvarioniene, C. Huber, K.P. Tsagarakis, E. Martinez-Lopez, S.M. Pagano, C. Vogelsang, G. Mascolo, Status of hormones and painkillers in wastewater effluents across several European states—considerations for the EU watch list concerning estradiols and diclofenac, *Environ. Sci. Pollut. Res. - Int.* 23 (2016) 12835–12866.
- [35] V. Likodimos, A. Chrysí, M. Calamiotou, C. Fernández-Rodríguez, J.M. Doña-Rodríguez, D.D. Dionysiou, P. Falaras, Microstructure and charge trapping assessment in highly reactive mixed phase TiO<sub>2</sub> photocatalysts, *Appl. Catal. B* 192 (2016) 242–252.
- [36] C. Salerno, P. Vergine, G. Berardi, A. Pollice, Influence of air scouring on the performance of a Self Forming Dynamic Membrane BioReactor (SFD MBR) for municipal wastewater treatment, *Bioresour. Technol.* 223 (2017) 301–306.
- [37] E. Rice, R. Baird, A. Eaton, L. Clesceri, Standard Methods for the Examination of Water and Wastewater, 22nd ed., APHA American Public Health Association, Washington, DC, 2012.
- [38] M.H.D. Othman, Z. Wu, N. Droushiotis, U. Doraswami, G. Kelsall, K. Li, Single-step fabrication and characterisation of electrolyte/anode dual-layer hollow fibres for micro-tubular solid oxide fuel cells, *J. Membr. Sci.* 351 (2010) 196–204.
- [39] H. Dzinun, M.H.D. Othman, A.F. Ismail, M.H. Puteh, M.A. Rahman, J. Jaafar, Photocatalytic degradation of nonylphenol using co-extruded dual-layer hollow fibre membranes incorporated with a different ratio of TiO<sub>2</sub>/PVDF, *React. Funct. Polym.* 99 (2016) 80–87.
- [40] H. Dzinun, M.H.D. Othman, A.F. Ismail, T. Matsuuura, M.H. Puteh, M.A. Rahman, J. Jaafar, Stability study of extruded dual layer hollow fibre membranes in a long operation photocatalysis process, *Polym. Test.* 68 (2018) 53–60.
- [41] T.E. Doll, F.H. Frimmel, Kinetic study of photocatalytic degradation of carbamazepine, clofibric acid, iomeprol and ipromide assisted by different TiO<sub>2</sub> materials—determination of intermediates and reaction pathways, *Water Res.* 38 (2004) 955–964.
- [42] Y. He, N.B. Sutton, H.H.H. Rijnaarts, A.A.M. Langenhoff, Degradation of pharmaceuticals in wastewater using immobilized TiO<sub>2</sub> photocatalysis under simulated

- solar irradiation, *Appl. Catal. B* 182 (2016) 132–141.
- [43] P. Asaithambi, R. Saravanathanthamizhan, M. Matheswaran, Comparison of treatment and energy efficiency of advanced oxidation processes for the distillery wastewater, *Int. J. Environ. Sci. Technol.* 12 (2015) 2213–2220.
- [44] M. Loos, EnviMass Version 3.5 LC-HRMS Trend Detection Workflow-R Package, (2018).
- [45] A. Detomaso, G. Mascolo, A. Lopez, Characterization of carbofuran photodegradation by-products by liquid chromatography/hybrid quadrupole time-of-flight mass spectrometry, *Rapid Commun. Mass Spectrom.* 19 (2005) 2193–2202.
- [46] V. Homem, L. Santos, Degradation and removal methods of antibiotics from aqueous matrices—a review, *J. Environ. Manage.* 92 (2011) 2304–2347.
- [47] C. Afonso-Olivares, C. Fernández-Rodríguez, R.J. Ojeda-González, Z. Sosa-Ferrera, J.J. Santana-Rodríguez, J.M.D. Rodríguez, Estimation of kinetic parameters and UV doses necessary to remove twenty-three pharmaceuticals from pre-treated urban wastewater by UV/H<sub>2</sub>O<sub>2</sub>, *J. Photochem. Photobiol. A Chem.* 329 (2016) 130–138.
- [48] O.S. Keen, N.G. Love, K.G. Linden, The role of effluent nitrate in trace organic chemical oxidation during UV disinfection, *Water Res.* 46 (2012) 5224–5234.
- [49] E. Lee, C.M. Glover, F.L. Rosario-Ortiz, Photochemical formation of hydroxyl radical from effluent organic matter: role of composition, *Environ. Sci. Technol.* 47 (2013) 12073–12080.
- [50] S. Chakraborty, S. Loutatidou, G. Palmisano, J. Kujawa, M.O. Mavukkandy, S. Al-Gharabli, E. Curcio, H.A. Arafat, Photocatalytic hollow fiber membranes for the degradation of pharmaceutical compounds in wastewater, *J. Environ. Chem. Eng.* 5 (2017) 5014–5024.
- [51] X. Liu, Y. Liu, S. Lu, W. Guo, B. Xi, Performance and mechanism into TiO<sub>2</sub>/Zeolite composites for sulfadiazine adsorption and photodegradation, *Chem. Eng. J.* 350 (2018) 131–147.
- [52] M.R. Hoffmann, S.T. Martin, W. Choi, D.W. Bahnemann, Environmental applications of semiconductor photocatalysis, *Chem. Rev.* 95 (1995) 69–96.
- [53] J. Romão, D. Barata, N. Ribeiro, P. Habibovic, H. Fernandes, G. Mul, High throughput screening of photocatalytic conversion of pharmaceutical contaminants in water, *Environ. Pollut.* 220 (2017) 1199–1207.
- [54] A. Ibadon, P. Fitzpatrick, Heterogeneous photocatalysis: recent advances and applications, *Catalysts* 3 (2013) 189.
- [55] D. Friedmann, C. Mendive, D. Bahnemann, TiO<sub>2</sub> for water treatment: parameters affecting the kinetics and mechanisms of photocatalysis, *Appl. Catal. B* 99 (2010) 398–406.
- [56] J. Bräme, M. Long, Q. Li, P. Alvarez, Inhibitory effect of natural organic matter or other background constituents on photocatalytic advanced oxidation processes: mechanistic model development and validation, *Water Res.* 84 (2015) 362–371.
- [57] U. Muhammad, A.A. Hamidi, Photocatalytic degradation of organic pollutants in water, in: N.M. Rashed (Ed.), *Organic Pollutants-Monitoring, Risk and Treatment*, IntechOpen Limited, London, 2013.
- [58] American Air and Water, UV Lamp Specifications, (2017) [http://www.americanairandwater.com/al/lamp\\_specs.htm](http://www.americanairandwater.com/al/lamp_specs.htm).
- [59] C. Guijas, J.R. Montenegro-Burke, X. Domingo-Almenara, A. Palermo, B. Warth, G. Hermann, G. Koellensperger, T. Huan, W. Uritboonthai, A.E. Aisporna, D.W. Wolan, M.E. Spilker, H.P. Benton, G. Siuzdak, METLIN: a technology platform for identifying knowns and unknowns, *Anal. Chem.* 90 (2018) 3156–3164.
- [60] G. Mascolo, A. Lopez, A. Detomaso, G. Lovecchio, Ion chromatography-electrospray mass spectrometry for the identification of low-molecular-weight organic acids during the 2,4-dichlorophenol degradation, *J. Chromatogr. A* 1067 (2005) 191–196.
- [61] C. Pastore, E. Barca, G. Del Moro, C. Di Iaconi, M. Loos, H.P. Singer, G. Mascolo, Comparison of different types of landfill leachate treatments by employment of nontarget screening to identify residual refractory organics and principal component analysis, *Sci. Total Environ.* 635 (2018) 984–994.